Flavour anomalies in $b \to s\ell^+\ell^-$ transitions at LHCb

Konstantinos A. Petridis

University of Bristol

November 2, 2021

Overview

- Introduction to Rare B decays
- Flavour Anomalies
- Interpretations
- Final Thoughts

Introduction

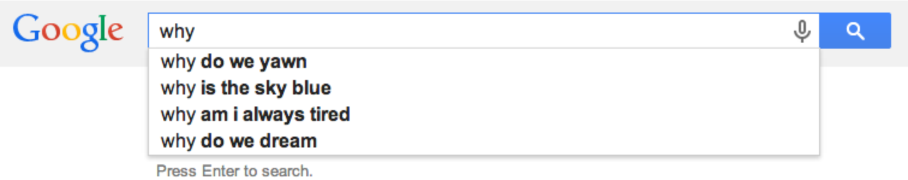

why

why **do we yawn**

why **is the sky blue**

why **am i always tired**

why **do we dream**

Press Enter to search.

- Why is there a hierarchy of fermion masses?
- Why do elements of the CKM matrix have a large spread?
- What is the origin of CP violation in the universe?
- What is the origin of dark matter?

→ SM is low-energy effective theory

What is the scale Λ where new physics shows up?

Experimental approaches

SM could be a low-energy effective theory of a more fundamental theory at higher energy scale with new particles, dynamics/symmetries.

Direct approach

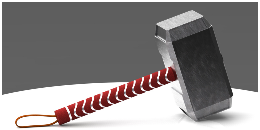

- Rely on high energy collisions to produce new particle(s) on-mass-shell, observed through their decay products

Indirect approach (typical of flavour)

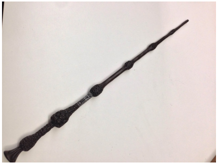

- New particles appear off-mass-shell in heavy flavour processes, leading to deviations from SM expectations

Indirect probe of high NP scales

Look at observables that:

1. The SM contribution is small
2. Can be measured to high precision
3. Can be predicted to high precision

→ Flavour Changing Neutral Currents in SM

- Loop level
- GIM suppressed
- Left-handed chirality

→ NP could violate any of these

$\Delta F = 1$ Rare B decays

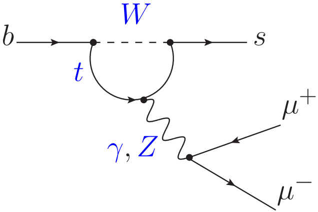

$\Delta F = 2$ B Mixing

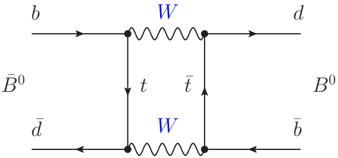

$B^+ \to K^+\ell^+\ell^-$ and related decays

- Occur through $b \to s\ell^+\ell^-$ transition and contain a hadron in the final state. e.g $B^+ \to K^+\ell^+\ell^-$, $B^0 \to K^{*0}\ell^+\ell^-$, $B_s \to \phi\mu^+\mu^-$, $\Lambda_b \to \Lambda^*\ell^+\ell^-$...

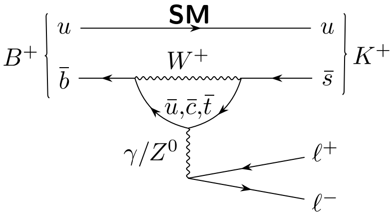

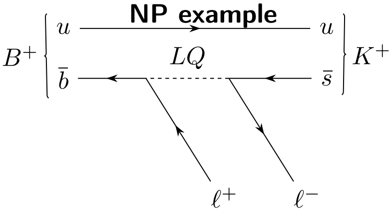

- Offer multitude of observables.

SM as effective theory

- "Integrate" out heavy ($m \geq m_W$) field(s) and introduce set of Wilson coefficients C_i, and operators $\mathcal{O}_i$ encoding short and long distance effects
- New physics enters at larger scale Λ_{NP}

$$\mathcal{H}_{eff} \approx -\frac{4G_F}{\sqrt{2}} V_{tb} V^*_{ts(d)} \sum_i C_i^{SM} \mathcal{O}_i^{SM} + \sum_{NP} \frac{c_{NP}}{\Lambda^2_{NP}} \mathcal{O}_{NP}$$

for 6 dim operators $\mathcal{O}_{NP}$

Sensitivity to New Physics

- Different decays probe different operators:

Operator $\mathcal{O}_i$	$B_{s(d)} \to X_{s(d)}\mu^+\mu^-$	$B_{s(d)} \to \mu^+\mu^-$	$B_{s(d)} \to X_{s(d)}\gamma$
$\mathcal{O}_7$ EM	✓		✓
$\mathcal{O}_9$ Vector dilepton	✓		
$\mathcal{O}_{10}$ Axial-vector dilepton	✓	✓	
$\mathcal{O}_{S,P}$ (Pseudo-)Scalar dilepton	(✓)	✓	

- Also include chirality flipped counterparts

Collider vs Flavour searches

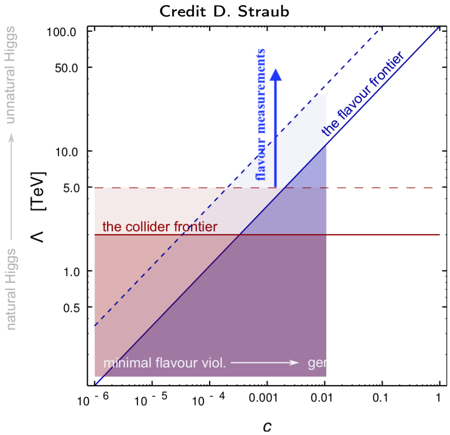

New Physics scale given current experiment and theory status in rare B decays:

$$\Lambda_9 \gtrsim (0.6 - 35)\ \text{TeV}$$
$$\Lambda_7 \gtrsim (1.5 - 90)\ \text{TeV}$$

depending on couplings and tree/loop level

- Rare B decay and flavour physics in general probes very high energy scales particularly for generic flavour couplings

Setting the scene

- LHC $\sigma_{b\bar{b}} = 460\,\mu\text{b}$ @ $\sqrt{s} = 13\,\text{TeV}$ (scale $\sim$ linear with $\sqrt{s}$)
- $\sigma_{b\bar{b}}$ in LHCb acceptance $\sim 100\,\mu\text{b}$
  - c.f $\sigma_{b\bar{b}} = 0.001\,\mu\text{b}$ @ B-factories

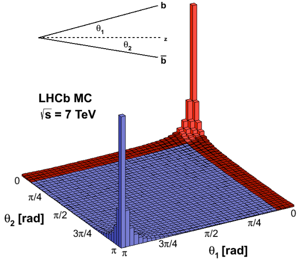

Run 2: 6fb^{-1} @ $\sqrt{s} = 13\text{TeV}$
Run 1: 3fb^{-1} @ $\sqrt{s} = 7, 8\text{TeV}$,

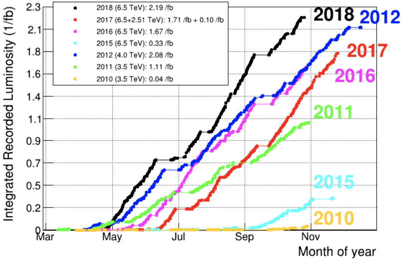

$L^{Max}_{inst} = 4 \times 10^{32}\text{cm}^{-2}\text{s}^{-1}$ (double the design value)

The LHCb detector

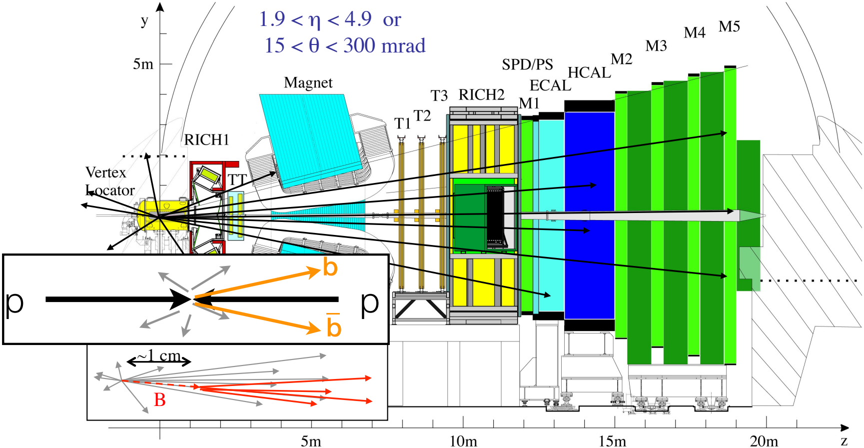

- UK responsible for VeLo and RICH systems
- *B*-lifetime means displaced secondary vertex

The LHCb trigger in Run 2

The challenge

- Only 1 in 200 pp inelastic events contain a *b*-quark
- Looking for *B*-hadron decays with $BF \sim 10^{-6} - 10^{-9}$

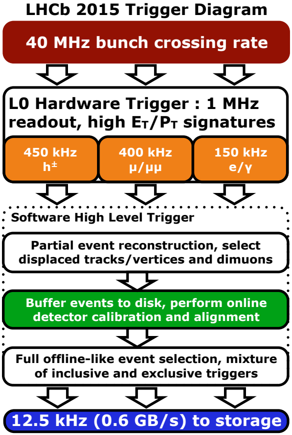

LHCb 2015 Trigger Diagram

40 MHz bunch crossing rate

L0 Hardware Trigger : 1 MHz readout, high E_T/P_T signatures

Software High Level Trigger

Partial event reconstruction, select displaced tracks/vertices and dimuons

Buffer events to disk, perform online detector calibration and alignment

Full offline-like event selection, mixture of inclusive and exclusive triggers

12.5 kHz (0.6 GB/s) to storage

Major development for Run 2:

- Buffer all events after HLT1 to perform calibrations and alignment
  - Determine calibration and alignment constants per fill (minutes)
  - Global offline-like reconstruction using these constants
  - Major step towards realising upgrade trigger strategy (see later)

→ More selective triggers e.g offline like particle ID in the trigger!

→ Physics measurement with data straight out of HLT2

- Output rate of HLT2 12.5kHz

Flavour Anomalies

Over the past decade we have observed a coherent set of tensions with SM predictions

In $b \to s\ell^+\ell^-$ transitions (FCNC)

1. **Branching Fractions**
   $B \to K^{(*)}\mu^+\mu^-$, $B_s \to \phi\mu^+\mu^-$, $\Lambda_b \to \Lambda\mu^+\mu^-$
2. **Angular analyses**
   $B \to K^{(*)}\mu^+\mu^-$, $\Lambda_b \to \Lambda\mu^+\mu^-$
3. **Lepton Flavour Universality involving μ/e ratios**
   $B^0 \to K^{*0}\ell^+\ell^-$, $B^+ \to K^+\ell^+\ell^-$

In $b \to c\ell\nu$ transitions (tree-level)

4. **Lepton Flavour Universality involving μ/τ ratios**
   $B \to D^{(*)}\ell\nu$

Flavour Anomalies

Over the past decade we have observed a coherent set of tensions with SM predictions

In $b \to s\ell^+\ell^-$ transitions (FCNC)

1. **Branching Fractions**
   $B \to K^{(*)}\mu^+\mu^-$, $B_s \to \phi\mu^+\mu^-$, $\Lambda_b \to \Lambda\mu^+\mu^-$

2. **Angular analyses**
   $B \to K^{(*)}\mu^+\mu^-$, $\Lambda_b \to \Lambda\mu^+\mu^-$

3. **Lepton Flavour Universality involving μ/e ratios**
   $B^0 \to K^{*0}\ell^+\ell^-$, $B^+ \to K^+\ell^+\ell^-$

In $b \to c\ell\nu$ transitions (tree-level)

4. Lepton Flavour Universality involving μ/τ ratios
   $B \to D^{(*)}\ell\nu$

Lepton Flavour Universality tests (I)

- In the SM couplings of gauge bosons to leptons are independent of lepton flavour
  → Branching fractions differ only by phase space and helicity-suppressed contributions

- Ratios of the form:

$$R_{K^{(*)}} := \frac{\mathcal{B}(B \to K^{(*)}\mu^+\mu^-)}{\mathcal{B}(B \to K^{(*)}e^+e^-)} \overset{\mathrm{SM}}{\cong} 1$$

- In SM free from QCD uncertainties affecting other observables
  → $\mathcal{O}(10^{-4})$ uncertainty [JHEP07(2007)040]
- Up to $\mathcal{O}(1\%)$ QED corrections [EPJC76(2016)8,440]

→ **Any significant deviation is a smoking gun for New Physics.**

Lepton Flavour Universality tests (II)

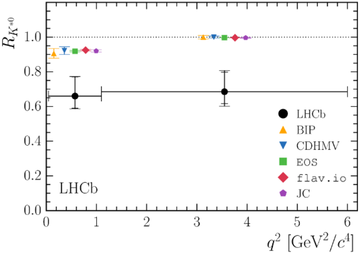

BaBar:[PRD86(2012)032012],Belle:[PRL103(2009)171801]

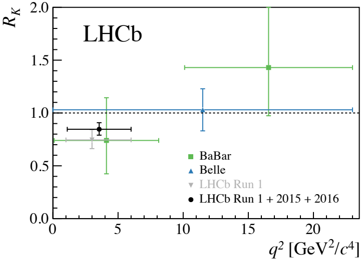

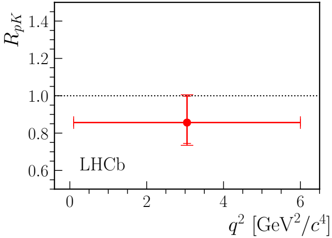

Left: $B^0 \to K^{*0}\ell^+\ell^-$ R_{K^*} 3fb^{-1}
[JHEP08(2017)055]

Right: $B^+ \to K^+\ell^+\ell^-$ R_K 5fb^{-1}
[PRL122(2019)191801]

Bottom: $\Lambda_b \to pK\ell^+\ell^-$ R_{pK} 4.7fb^{-1}
[JHEP05(2020)040]

($q^2 \equiv$ dilepton invariant mass squared)

R_K with the full LHCb dataset

$$R_K = \frac{\int_{1.1\,\mathrm{GeV}^2}^{6.0\,\mathrm{GeV}^2} \frac{\mathrm{d}\mathcal{B}(B^+\to K^+\mu^+\mu^-)}{\mathrm{d}q^2}\mathrm{d}q^2}{\int_{1.1\,\mathrm{GeV}^2}^{6.0\,\mathrm{GeV}^2} \frac{\mathrm{d}\mathcal{B}(B^+\to K^+e^+e^-)}{\mathrm{d}q^2}\mathrm{d}q^2}$$

Measurement performed in $1.1 < q^2 < 6.0\,\mathrm{GeV}^2/c^4$

- Previous measurement [PRL122(2019)191801] used $5\,\mathrm{fb}^{-1}$ of data.
  $3\,\mathrm{fb}^{-1}$ of Run1
  $2\,\mathrm{fb}^{-1}$ of Run2 in 2015 and 2016
- This update:
  → Add remaining $4\,\mathrm{fb}^{-1}$ of Run2 in 2017 and 2018 .
  → $9\,\mathrm{fb}^{-1}$ in total.
  → Doubling the number of B's as previous analysis.
- Follow the same analysis strategy as our previous measurement.

Electrons vs muons (I)

- Electrons lose a large fraction of their energy through Bremsstrahlung in detector material

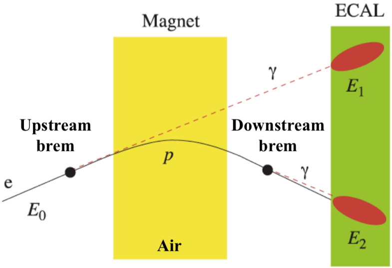

- Most electrons will emit one energetic photon the before magnet.

  → Look for photon clusters in the calorimeter ($E_T > 75\,\mathrm{MeV}$) compatible with electron direction before magnet.

  → Recover brem energy loss by "adding" the cluster energy back to the electron momentum.

Electrons vs muons (II)

- Even after the Bremsstrahlung recovery electrons still have degraded mass and q^2 resolution

From previous result, LHCb [PRL122(2019)191801]

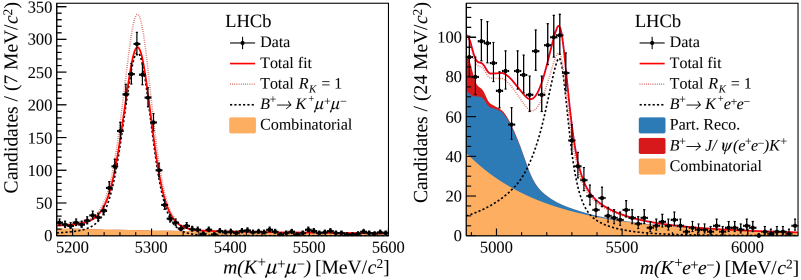

- L0 calorimeter trigger requires higher thresholds, than L0 muon trigger, due to high occupancy.

  → Use 3 exclusive trigger categories for e^+e^- final states

  1. $e^\pm$ from signal-B; 2. $K^\pm$ from signal-B; 3. rest of event

- Particle ID and tracking efficiency larger for muons than electrons

Electrons vs muons (II)

- Even after the Bremsstrahlung recovery electrons still have degraded mass and q^2 resolution

From previous result, LHCb [PRL122(2019)191801]

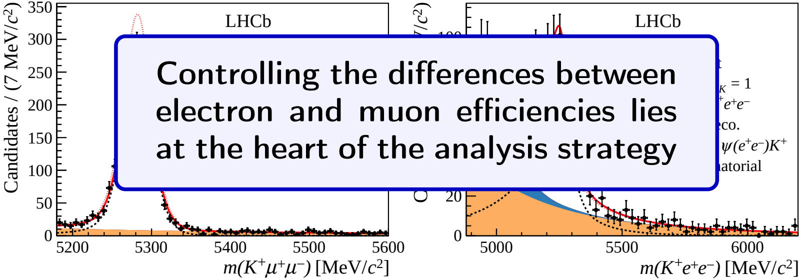

Controlling the differences between electron and muon efficiencies lies at the heart of the analysis strategy

- L0 calorimeter trigger requires higher thresholds, than L0 muon trigger, due to high occupancy.

  → Use 3 exclusive trigger categories for e^+e^- final states

  1. $e^\pm$ from signal-B; 2. $K^\pm$ from signal-B; 3. rest of event

- Particle ID and tracking efficiency larger for muons than electrons

Measurement Strategy

$$R_K = \frac{\mathcal{B}(B^+ \to K^+ \mu^+ \mu^-)}{\mathcal{B}(B^+ \to K^+ J/\psi(\mu^+ \mu^-))} \Bigg/ \frac{\mathcal{B}(B^+ \to K^+ e^+ e^-)}{\mathcal{B}(B^+ \to K^+ J/\psi(e^+ e^-))} = \frac{N^{\rm rare}_{\mu^+\mu^-}\ \varepsilon^{J/\psi}_{\mu^+\mu^-}}{N^{J/\psi}_{\mu^+\mu^-}\ \varepsilon^{\rm rare}_{\mu^+\mu^-}} \times \frac{N^{J/\psi}_{e^+e^-}\ \varepsilon^{\rm rare}_{e^+e^-}}{N^{\rm rare}_{e^+e^-}\ \varepsilon^{J/\psi}_{e^+e^-}}$$

→ R_K is measured as a **double ratio** to cancel out most systematics

- Rare and J/ψ modes share identical selections apart from cut on q^2
- Yields determined from a fit to the invariant mass of the final state particles
- Efficiencies computed using simulation that is calibrated with control channels in data

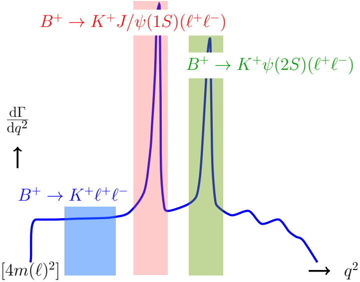

($q^2 \equiv$ dilepton invariant mass squared)

Selection and backgrounds

- As in our previous measurement, use particle ID requirements and mass vetoes to suppress peaking backgrounds from exclusive B-decays to negligible levels
    - ▷ Backgrounds of e.g $B^+ \to \bar{D}^0(\to K^+e^-\nu)e^+\bar{\nu}$: cut on $m_{K^+e^-} > m_{D^0}$
    - ▷ Mis-ID backgrounds, e.g. $B \to K\pi^+_{(\to e^+)}\pi^-_{(\to e^-)}$: cut on electron PID
- Multivariate selection to reduce combinatorial background and improve signal significance (BDT)

Residual backgrounds suppressed by choice of $m(K^+\ell^+\ell^-)$ window

- $B^+ \to K^+J/\psi(e^+e^-)$
- Partially reconstructed dominated by $B \to K^+\pi^-e^+e^-$ decays
- Model in fit by constraining their fractions between trigger categories and calibrating simulated templates from data.

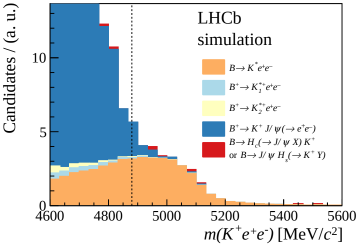

Cross-check our estimates using control regions in data and changing $m(K^+\ell^+\ell^-)$ window in fit

Efficiency calibration

Following identical procedure to our previous measurement, the simulation is calibrated based on control data for the following quantities:

- Trigger efficiency.
- Particle identification efficiency.
- B^+ kinematics.
- Resolutions of q^2 and $m(K^+e^+e^-)$.

Verify procedure through host of cross-checks.

Cross-check: Measurement of $r_{J/\psi}$

LHCb [arXiv:2103.11769]

- To ensure that the efficiencies are under control, check

$$r_{J/\psi} = \frac{\mathcal{B}(B^+ \to K^+ J/\psi(\mu^+\mu^-))}{\mathcal{B}(B^+ \to K^+ J/\psi(e^+e^-))} = 1,$$

known to be true within 0.4% [Particle Data Group].
→ Very stringent check, as it requires direct control of muons vs electrons.

- Result:

$$r_{J/\psi} = 0.981 \pm 0.020\ (\mathrm{stat} + \mathrm{syst})$$

- Checked that the value of $r_{J/\psi}$ is compatible with unity for new and previous datasets and in all trigger samples.

Cross-check: $r_{J/\psi}$ as a function of kinematics

LHCb [arXiv:2103.11769]

- Test efficiencies are understood in all kinematic regions by checking $r_{J/\psi}$ is flat in all variables examined.

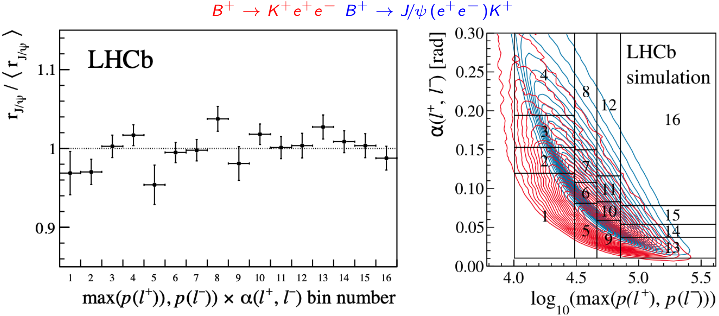

- Flatness of $r_{J/\psi}$ 2D plots gives confidence that efficiencies are understood across entire decay phase-space.

  → If take departure from flatness as genuine rather than fluctuations (accounting for rare-mode kinematics) bias expected on R_K is 0.1%

Cross-check: Measurement of $R_{\psi(2S)}$

LHCb [arXiv:2103.11769]

Measurement of the double ratio

$$R_{\psi(2S)} = \frac{\mathcal{B}(B^+ \to K^+\psi(2S)(\mu^+\mu^-))}{\mathcal{B}(B^+ \to K^+J/\psi(\mu^+\mu^-))} \Bigg/ \frac{\mathcal{B}(B^+ \to K^+\psi(2S)(e^+e^-))}{\mathcal{B}(B^+ \to K^+J/\psi(e^+e^-))}$$

- Independent validation of double-ratio procedure at q^2 away from J/ψ
- Result well compatible with unity:

$$R_{\psi(2S)} = 0.997 \pm 0.011\ (\mathrm{stat} + \mathrm{syst})$$

→ can be interpreted as world's best LFU test in $\psi(2S) \to \ell^+\ell^-$

Fit to new $B^+ \to \psi(2S)(\ell^+\ell^-)K^+$ data

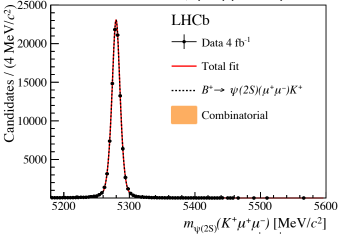

Use $\psi(2S)$ constrained $m(K^+\ell^+\ell^-)$

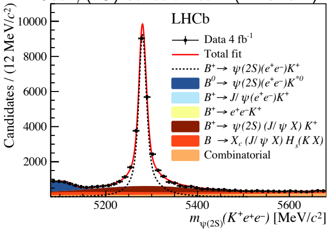

Systematic uncertainties

LHCb [arXiv:2103.11769]

Dominant sources: ~ 1**%**

- Choice of fit model
  - Associated signal and partially reconstructed background shape
- Statistics of calibration samples
  - Bootstrapping method that takes into account correlations between calibration samples and final measurement

Sub-dominant sources: ~ 1**‰**

- Efficiency calibration

→ Dependence on tag definition and trigger biases
→ Precision of the q^2 and $m(K^+e^+e^-)$ smearing factors
→ Inaccuracies in material description in simulation
...

Total relative systematic of 1.5% in the final R_K measurement
→ Expected to be statistically dominated

Measuring R_K

LHCb [arXiv:2103.11769]

- R_K is extracted as a parameter from an unbinned maximum likelihood fit to $m(K^+\mu^+\mu^-)$ and $m(K^+e^+e^-)$ distributions in $B^+ \to K^+\ell^+\ell^-$ and $B^+ \to J/\psi(\ell^+\ell^-)K^+$ decays

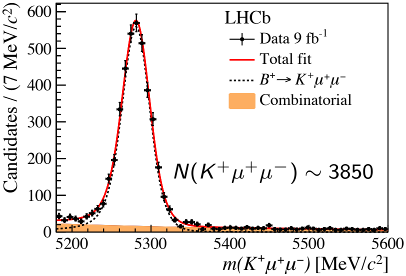

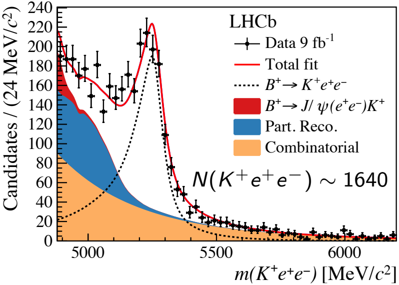

- Correlated uncertainties on efficiency ratios included as multivariate constraint in likelihood

R_K with full Run1 and Run2 dataset

LHCb [arXiv:2103.11769]**Submitted to Nature Physics**

$$R_K = 0.846\ ^{+0.042}_{-0.039}\ (\mathrm{stat})\ ^{+0.013}_{-0.012}\ (\mathrm{syst})$$

- *p*-value under SM hypothesis: 0.0010 → Evidence of LFU violation at 3.1σ
- Compatibility with the SM obtained by integrating the profiled likelihood as a function of R_K above 1
  - Taking into account the 1% theory uncertainty on R_K [EPJC76(2016)8,440]

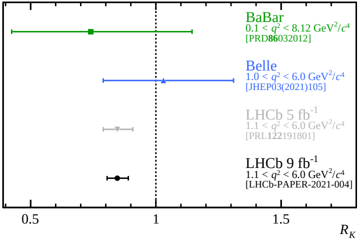

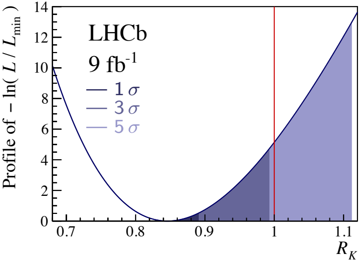

R_K with full Run1 and Run2 dataset

LHCb [arXiv:2103.11769]**Submitted to Nature Physics**

$$R_K = 0.846\ ^{+0.042}_{-0.039}\ (\text{stat})\ ^{+0.013}_{-0.012}\ (\text{syst})$$

- p-value under SM hypothesis: 0.0010
  $\rightarrow$ Evidence of LFU violation at 3.1σ
- Using R_K and previous measurement of $\mathcal{B}(B^+ \rightarrow K^+\mu^+\mu^-)$ [JHEP06(2014)133] determine $\mathcal{B}(B^+ \rightarrow K^+e^+e^-)$.
- Suggests electrons are more SM-like than muons.

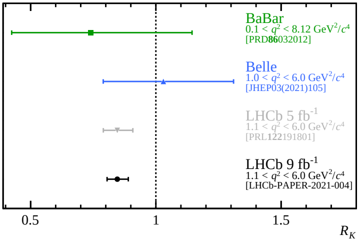

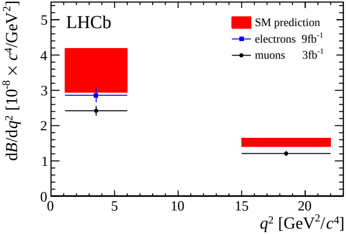

$$\frac{\mathrm{d}\mathcal{B}(B^+\rightarrow K^+e^+e^-)}{\mathrm{d}q^2} = (28.6\ ^{+1.5}_{-1.4}(\text{stat})\ \pm 1.4(\text{syst})) \times 10^{-9}\ c^4/\,\text{GeV}^2.$$

NEW: $R_{K^{*+}}$ and R_{K_S}

[LHCb-PAPER-2021-038]

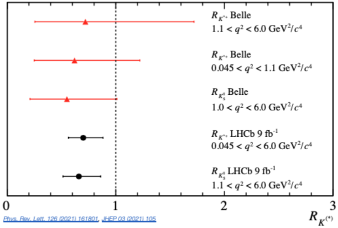

- LFU tests with $B^+ \to K^{*+}(\to K_S\pi^+)\ell^+\ell^-$ and $B^0 \to K_S\ell^+\ell^-$ with $K_S \to \pi^+\pi^-$
- Analysis procedure identical to R_K
  - $R_{K^{*+}}$ measured in $0.045 < q^2 < 6\,\mathrm{GeV}^2/c^4$
- Combined significance wrt SM 2σ

[Credit H. Cliff CERN seminar]

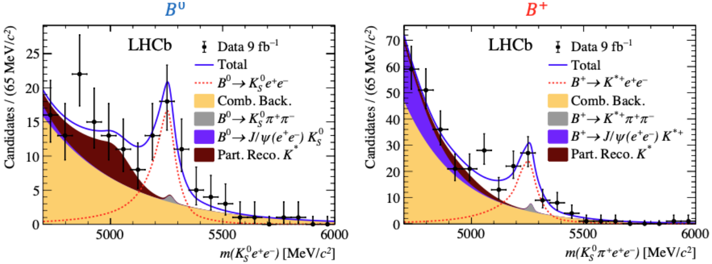

$B^0 \to K^0_S \ell^+\ell^-$ significance: 5.3σ

$B^+ \to K^{*+}\ell^+\ell^-$ significance: 6.0σ

Flavour Anomalies

Over the past decade we have observed a coherent set of tensions with SM predictions

In $b \to s\ell^+\ell^-$ transitions (FCNC)

1. **Branching Fractions**
   $\boldsymbol{B \to K^{(*)}\mu^+\mu^-}$, $\boldsymbol{B_s \to \phi\mu^+\mu^-}$, $\boldsymbol{\Lambda_b \to \Lambda\mu^+\mu^-}$
2. **Angular analyses**
   $\boldsymbol{B \to K^{(*)}\mu^+\mu^-}$, $\boldsymbol{\Lambda_b \to \Lambda\mu^+\mu^-}$
3. **Lepton Flavour Universality involving μ/e ratios**
   $B^0 \to K^{*0}\ell^+\ell^-$, $B^+ \to K^+\ell^+\ell^-$

In $b \to c\ell\nu$ transitions (tree-level)

4. Lepton Flavour Universality involving μ/τ ratios
   $B \to D^{(*)}\ell\nu$

1. Decay Rates

- Measurements consistently below theory predictions at low $q^2 \equiv m^2_{\ell\ell}$ for many $b \to s\mu^+\mu^-$ decays

[JHEP06(2014)133]

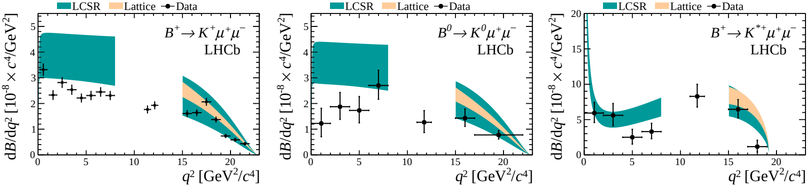

$B^0 \to K^{*0}\mu^+\mu^-$ [JHEP11(2016)047], $\Lambda_b \to \Lambda\mu^+\mu^-$ [JHEP06(2015)115] $B_s \to \phi\mu^+\mu^-$ [JHEP09(2015)179]

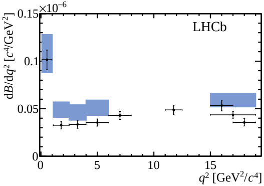

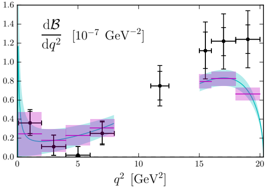

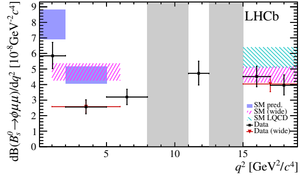

- SM predictions suffer from large hadronic uncertainties

2. Angular analyses of $B \to K^{*}\mu^{+}\mu^{-}$

- Large number of observables offering complementary constraints on NP compared to BF's
- Orthogonal experimental systematics and more precise theory predictions

Left: $B^{0} \to K^{*0}\mu^{+}\mu^{-}$ **[PRL125011802(2020)], Right:** $B^{+} \to K^{*+}\mu^{+}\mu^{-}$ **[arXiv:2012.13241]**

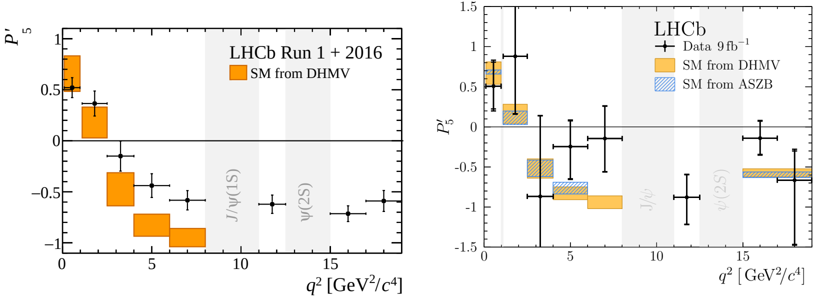

- Combination of all angular observables suggests $\sim 3\sigma$ tension with SM predictions in each channel

Putting it all together

- Combination all $b \to s\ell^+\ell^-$ measurements
  - $> 6\sigma$ from SM
- $B_s \to \mu^+\mu^-$ and LFU observables have very clean theory predictions.
  - $\sim 4.5\sigma$ from SM
- Measurements point to new vector coupling (C_9^μ)

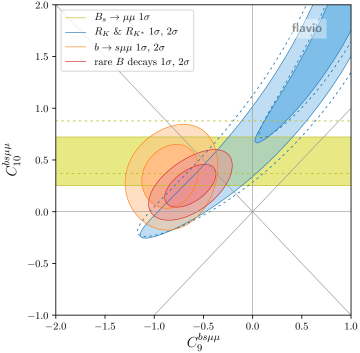

- $B \to K^{(*)}\mu^+\mu^-$ BF and angular observables potentially suffer from underestimated hadronic uncertainties.

  → Can extract hadronic contributions directly from data
  [Bobeth et al EPJC(2018)78:451], [Pomery, KP et al EPJC(2018)78:453]

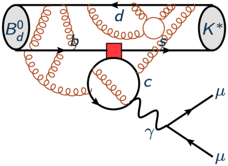

Putting it all together

- Combination all $b \to s\ell^+\ell^-$ measurements
  - $> 6\sigma$ from SM
- $B_s \to \mu^+\mu^-$ and LFU observables have very clean theory predictions.
  - $\sim 4.5\sigma$ from SM
- Measurements point to new vector coupling (C_9^μ)

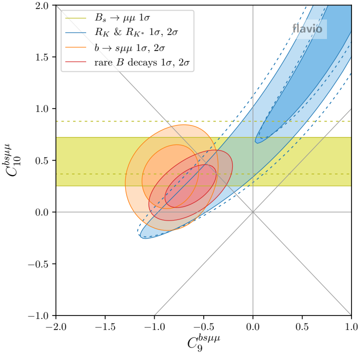

- Links to $(g-2)_\mu$: SM predictions aside, there are models that can accommodate both anomalies

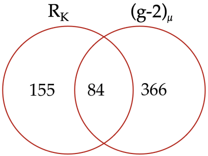

Papers citing new results
(as of 30/10/2021)

Highly predictive models

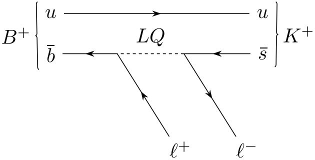

$\rightarrow$ Leptoquarks Isidori et al [JHEP1907(2019)168,JHEP10(2018)148,PLB(2018)317], Greljo et al [JHEP07(2015)142], Buttazzo et al [JHEP08(2016)035]...

Models that address anomalies can also explain hierarchical structure of quark and lepton mass matrices Isidori et al [PLB(2018)317].

High energy signatures

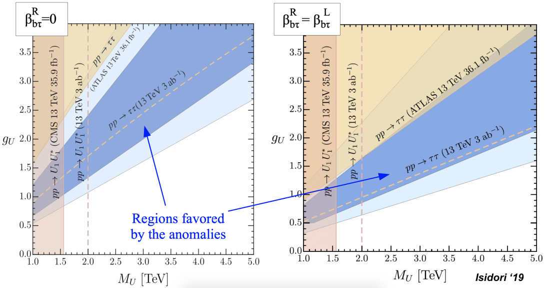

Isidori '19

- With 300ab^{-}1 $pp \to \tau\tau$ ATLAS and CMS can probe significant fraction of parameter space

Highly predictive models

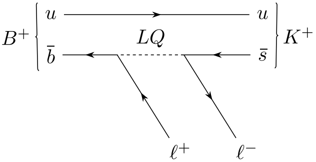

→ Leptoquarks Isidori et al [JHEP1907(2019)168,JHEP10(2018)148,PLB(2018)317], Greljo et al [JHEP07(2015)142], Buttazzo et al [JHEP08(2016)035]...

Models that address anomalies can also explain hierarchical structure of quark and lepton mass matrices Isidori et al [PLB(2018)317].

Low energy signatures

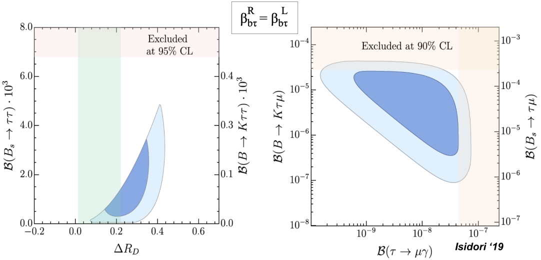

Isidori '19

- Huge enhancement of $b \to s\tau\tau$ and $b \to s\tau\mu$ that LHCb and Belle2 will be sensitive to soon

Outlook

Many more measurements underway with full LHCb dataset

- R_{K^*}, R_{pK} update, R_{ϕ}, $R_{K^{*+}}$...
- R_K and R_{K^*} at high q^2.
- Angular analyses of $B \to K^{(*)}e^+e^-$ and $B \to K^{(*)}\mu^+\mu^-$ decays.
- Further validation of our understanding of reconstruction effects at low q^2.
- $b \to s\tau\tau$ and LFV measurements with τ's
- ...

$\to$ Current dataset will offer clearer picture

For a definitive understanding, Run3 is imperative.

Input from our LHC and Belle2 colleagues is important.

Final thought: Naturalness' loss → Flavour's gain

- Lack of New Physics in direct searches lifts requirement of MFV
  - Large Λ_{NP} reach from flavour
- Without guidance on scale of New Physics, Flavour measurements are key!

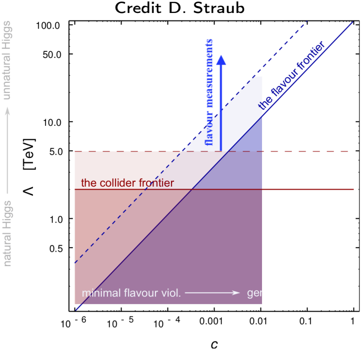
Credit D. Straub

$b \to s\ell\ell$	CKM+Loop	CKM+Tree	$\mathcal{O}(1)$+Loop	$\mathcal{O}(1)$+Tree
$\Lambda_{NP}^{9(10)(')}$(TeV)	~ 2	~ 10	~ 20	~ 100
$\Lambda_{NP}^{7(')}$(TeV)	~ 5	~ 20	~ 60	~ 300

my own guesstimates by LHCb PhaseII

Backup

Control mode fits

LHCb [arXiv:2103.11769]

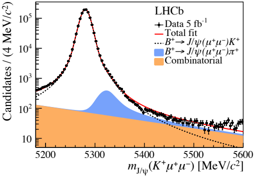

Previous data

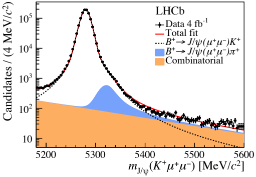

New data

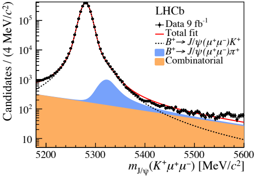

Total data

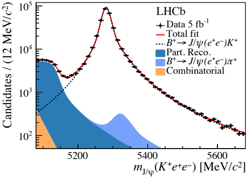

Previous data

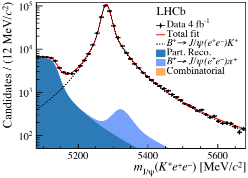

New data

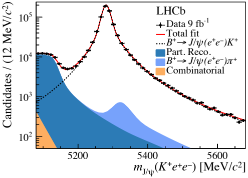

Total data

Signal Lineshape

- The $m(K^+\ell^+\ell^-)$ distributions of the rare mode are obtained from simulated decays, calibrating the peak and width of the distribution using $B^+ \to J/\psi(\ell^+\ell^-)K^+$ data.

- In the subsequent fit to the rare mode the $m(K^+\ell^+\ell^-)$ lineshape is fixed.

- The q^2 scale/resolution in the simulation is corrected using the same procedure
  $\to$ the efficiency of the q^2 cut is calibrated from the data

$B^+ \to K^+\ell^+\ell^-$

[PRL122(2019)191801]

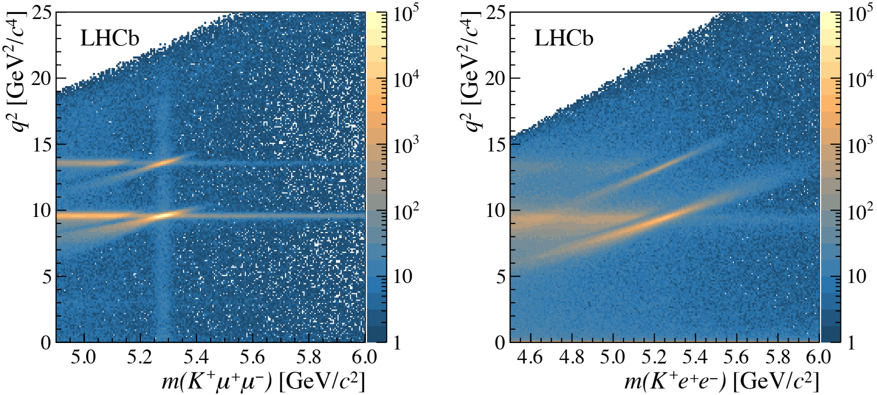

Semileptonic vetos

LHCb [arXiv:2103.11769]

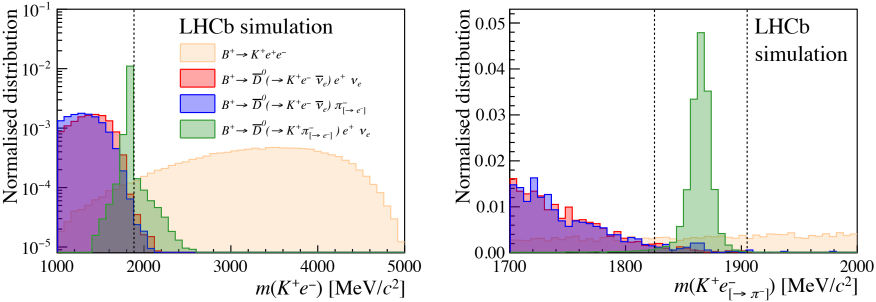

Parameter overlap (I)

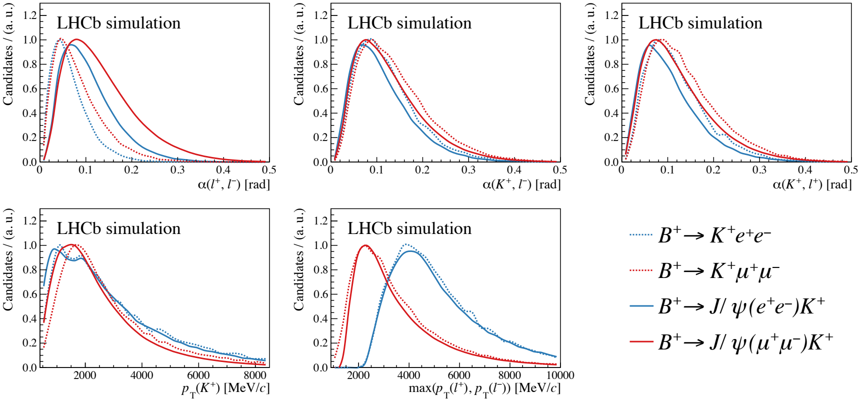

Parameter overlap (II)

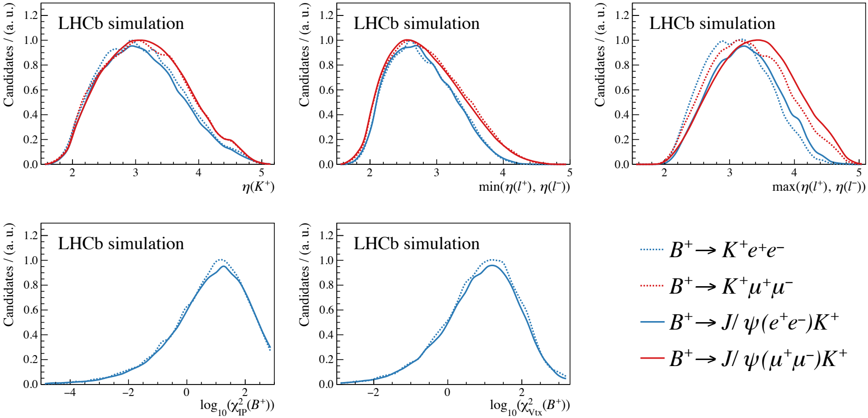

Efficiency calibration

Ratio of efficiencies determined with simulation carefully calibrated using control channels selected from data:

- Particle ID calibration
  - Tune particle ID variables for diff. particle species using kinematically selected calibration samples ($D^{*+} \to D^0(K^-\pi^+)\pi^+$...) [EPJ T&I(2019)6:1]
- Calibration of q^2 and $m(K^+e^+e^-)$ resolutions
  - Use fit to $m(J/\psi)$ to smear q^2 in simulation to match that in data
- Calibration of B^+ kinematics
- Trigger efficiency calibration

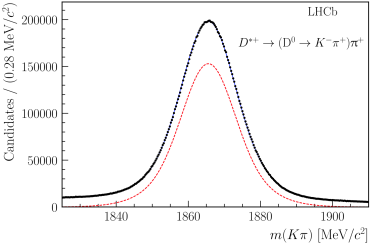

Calibration of B^+ kinematics

- Calibrate the simulation so that it describes correctly the kinematics of the B^+'s produced at LHCb.
- Compare distributions in data and simulation using $B^+ \to K^+ J/\psi(\ell^+\ell^-)$ candidates.
- Iterative reweighing of $p_T(B^+) \times \eta(B^+)$, but also the vertex quality and the significance of the B^+ displacement.

none

$\mu\mu$ `L0Muon`, nominal

$\mu\mu$ `L0TIS`

ee `L0Electron`

$VTX\chi^2$: ee `L0Electron`, $p_T(B)\times\eta(B)$, $IP\chi^2$: $\mu\mu$ `L0Muon`

[PRL 122 (2019) 191801]

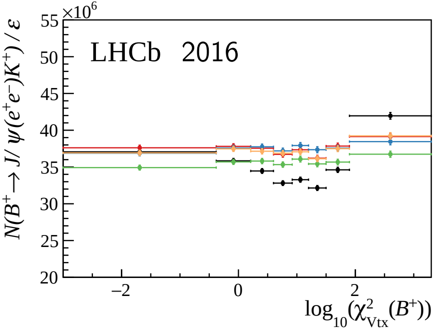

→ Systematic uncertainty from RMS between all these weights

Trigger efficiency

The trigger efficiency is computed in data using $B^+ \to K^+ J/\psi(\ell^+\ell^-)$ decays through a tag-and-probe method

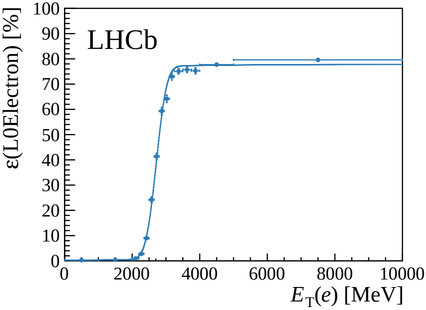

Especially for the electron samples, need to take into consideration some subtleties:

- dependence on how the calibration sample is selected,
- correlation between the two leptons in the signal.

Repeat calibration with different samples/different requirements on the accompanying lepton

→ Associated systematic in the ratio of efficiencies is small

Efficiency calibration summary

- After calibration, very good data/MC agreement in all key observables

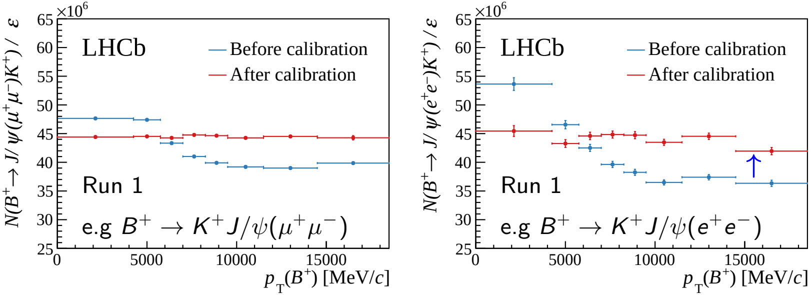

Maximal effect of turning off corrections results in relative shift R_K $(+3 \pm 1)\%$ compared to 20% in $r_{J/\psi}$.
Demonstrates the robustness of the double-ratio method in suppressing systematic biases that affect the resonant and nonresonant decay modes similarly.

Trigger strategy

[Credit: Dan Moise]

Same approach as in the previous analysis:

- for $\mu\mu$ channels, trigger on muons: `L0Muon`
- for *ee* channels, use three exclusive trigger categories: `L0Electron`, `L0Hadron`, `L0TIS`
- systematics calculated and cross-checks performed for each trigger individually

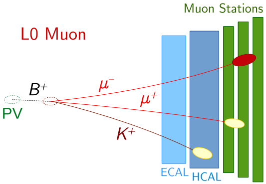

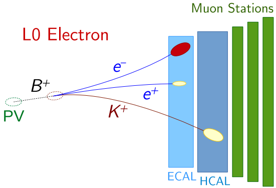

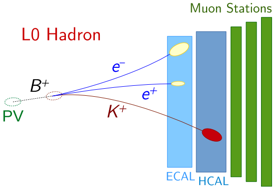

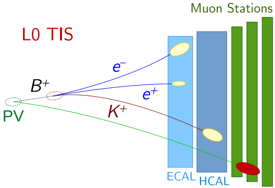

Conclusions

Using the full LHCb dataset to date, presented:

1. Single most precise measurement of $\mathcal{B}(B_s^0 \to \mu^+\mu^-)$, improved precision on $\tau_{\mu^+\mu^-}$ and first every limit on $B_s^0 \to \mu^+\mu^-\gamma$
2. Updated R_K measurement → 3.1σ departure from LFU!
   → Reframing discussion on flavour anomalies

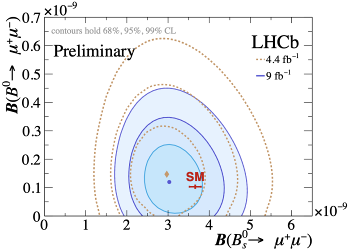

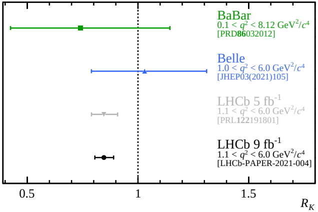

Complementarity between R_K and $\mathcal{B}(B_s^0 \to \mu^+\mu^+)$ measurements crucial moving forward.

"...perhaps the end of the beginning."

2. Angular analysis of $B^0 \to K^{*0}\mu^+\mu^-$

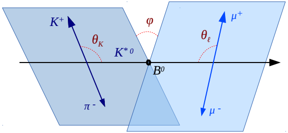

- Differential decay rate of $B^0 \to K^{*0}\mu^+\mu^-$ and $\bar{B}^0 \to \bar{K}^{*0}\mu^+\mu^-$:

$$\frac{\mathrm{d}^4\Gamma[\overline{B}^0 \to \overline{K}^{*0}\mu^+\mu^-]}{\mathrm{d}q^2\,\mathrm{d}\vec{\Omega}} = \frac{9}{32\pi}\sum_i I_i(q^2) f_i(\vec{\Omega}) \quad \text{and}$$
$$\frac{\mathrm{d}^4\bar{\Gamma}[B^0 \to K^{*0}\mu^+\mu^-]}{\mathrm{d}q^2\,\mathrm{d}\vec{\Omega}} = \frac{9}{32\pi}\sum_i \bar{I}_i(q^2) f_i(\vec{\Omega}) \ ,$$

- I_i: bilinear combinations of 6 P-wave and 2 S-wave helicity amplitudes (since K^{*0} can be found in $J = 1$ and $J = 0$)
- Reparametrise distribution in terms of:

$$S_i = (I_i + \bar{I}_i) \Big/ \left(\frac{\mathrm{d}\Gamma}{\mathrm{d}q^2} + \frac{\mathrm{d}\bar{\Gamma}}{\mathrm{d}q^2}\right) \quad \text{and}$$
$$A_i = (I_i - \bar{I}_i) \Big/ \left(\frac{\mathrm{d}\Gamma}{\mathrm{d}q^2} + \frac{\mathrm{d}\bar{\Gamma}}{\mathrm{d}q^2}\right) .$$

- Determine 8 S_i and 8 A_i for P-wave K^{*0} through a quasi 4D angular and $m_{K\pi}$ fit in bins of q^2

What are these I_is I hear you ask?

i	I_i	f_i
$1s$	$\frac{3}{4}\left[\lvert\mathcal{A}_{\parallel}^{\mathrm{L}}\rvert^2 + \lvert\mathcal{A}_{\perp}^{\mathrm{L}}\rvert^2 + \lvert\mathcal{A}_{\parallel}^{\mathrm{R}}\rvert^2 + \lvert\mathcal{A}_{\perp}^{\mathrm{R}}\rvert^2\right]$	$\sin^2\theta_K$
$1c$	$\lvert\mathcal{A}_{0}^{\mathrm{L}}\rvert^2 + \lvert\mathcal{A}_{0}^{\mathrm{R}}\rvert^2$	$\cos^2\theta_K$
$2s$	$\frac{1}{4}\left[\lvert\mathcal{A}_{\parallel}^{\mathrm{L}}\rvert^2 + \lvert\mathcal{A}_{\perp}^{\mathrm{L}}\rvert^2 + \lvert\mathcal{A}_{\parallel}^{\mathrm{R}}\rvert^2 + \lvert\mathcal{A}_{\perp}^{\mathrm{R}}\rvert^2\right]$	$\sin^2\theta_K\cos 2\theta_l$
$2c$	$-\lvert\mathcal{A}_{0}^{\mathrm{L}}\rvert^2 - \lvert\mathcal{A}_{0}^{\mathrm{R}}\rvert^2$	$\cos^2\theta_K\cos 2\theta_l$
3	$\frac{1}{2}\left[\lvert\mathcal{A}_{\perp}^{\mathrm{L}}\rvert^2 - \lvert\mathcal{A}_{\parallel}^{\mathrm{L}}\rvert^2 + \lvert\mathcal{A}_{\perp}^{\mathrm{R}}\rvert^2 - \lvert\mathcal{A}_{\parallel}^{\mathrm{R}}\rvert^2\right]$	$\sin^2\theta_K\sin^2\theta_l\cos 2\phi$
4	$\sqrt{\frac{1}{2}}\mathrm{Re}(\mathcal{A}_{0}^{\mathrm{L}}\mathcal{A}_{\parallel}^{\mathrm{L}*} + \mathcal{A}_{0}^{\mathrm{R}}\mathcal{A}_{\parallel}^{\mathrm{R}*})$	$\sin 2\theta_K\sin 2\theta_l\cos\phi$
5	$\sqrt{2}\mathrm{Re}(\mathcal{A}_{0}^{\mathrm{L}}\mathcal{A}_{\perp}^{\mathrm{L}*} - \mathcal{A}_{0}^{\mathrm{R}}\mathcal{A}_{\perp}^{\mathrm{R}*})$	$\sin 2\theta_K\sin\theta_l\cos\phi$
$6s$	$2\mathrm{Re}(\mathcal{A}_{\parallel}^{\mathrm{L}}\mathcal{A}_{\perp}^{\mathrm{L}*} - \mathcal{A}_{\parallel}^{\mathrm{R}}\mathcal{A}_{\perp}^{\mathrm{R}*})$	$\sin^2\theta_K\cos\theta_l$
7	$\sqrt{2}\mathrm{Im}(\mathcal{A}_{0}^{\mathrm{L}}\mathcal{A}_{\parallel}^{\mathrm{L}*} - \mathcal{A}_{0}^{\mathrm{R}}\mathcal{A}_{\parallel}^{\mathrm{R}*})$	$\sin 2\theta_K\sin\theta_l\sin\phi$
8	$\sqrt{\frac{1}{2}}\mathrm{Im}(\mathcal{A}_{0}^{\mathrm{L}}\mathcal{A}_{\perp}^{\mathrm{L}*} + \mathcal{A}_{0}^{\mathrm{R}}\mathcal{A}_{\perp}^{\mathrm{R}*})$	$\sin 2\theta_K\sin 2\theta_l\sin\phi$
9	$\mathrm{Im}(\mathcal{A}_{\parallel}^{\mathrm{L}*}\mathcal{A}_{\perp}^{\mathrm{L}} + \mathcal{A}_{\parallel}^{\mathrm{R}*}\mathcal{A}_{\perp}^{\mathrm{R}})$	$\sin^2\theta_K\sin^2\theta_l\sin 2\phi$
10	$\frac{1}{3}\left[\lvert\mathcal{A}_{\mathrm{S}}^{\mathrm{L}}\rvert^2 + \lvert\mathcal{A}_{\mathrm{S}}^{\mathrm{R}}\rvert^2\right]$	1
11	$\sqrt{\frac{4}{3}}\mathrm{Re}(\mathcal{A}_{\mathrm{S}}^{\mathrm{L}}\mathcal{A}_{0}^{\mathrm{L}*} + \mathcal{A}_{\mathrm{S}}^{\mathrm{R}}\mathcal{A}_{0}^{\mathrm{R}*})$	$\cos\theta_K$
12	$-\frac{1}{3}\left[\lvert\mathcal{A}_{\mathrm{S}}^{\mathrm{L}}\rvert^2 + \lvert\mathcal{A}_{\mathrm{S}}^{\mathrm{R}}\rvert^2\right]$	$\cos 2\theta_l$
13	$-\sqrt{\frac{4}{3}}\mathrm{Re}(\mathcal{A}_{\mathrm{S}}^{\mathrm{L}}\mathcal{A}_{0}^{\mathrm{L}*} + \mathcal{A}_{\mathrm{S}}^{\mathrm{R}}\mathcal{A}_{0}^{\mathrm{R}*})$	$\cos\theta_K\cos 2\theta_l$
14	$\sqrt{\frac{2}{3}}\mathrm{Re}(\mathcal{A}_{\mathrm{S}}^{\mathrm{L}}\mathcal{A}_{\parallel}^{\mathrm{L}*} + \mathcal{A}_{\mathrm{S}}^{\mathrm{R}}\mathcal{A}_{\parallel}^{\mathrm{R}*})$	$\sin\theta_K\sin 2\theta_l\cos\phi$
15	$\sqrt{\frac{8}{3}}\mathrm{Re}(\mathcal{A}_{\mathrm{S}}^{\mathrm{L}}\mathcal{A}_{\perp}^{\mathrm{L}*} - \mathcal{A}_{\mathrm{S}}^{\mathrm{R}}\mathcal{A}_{\perp}^{\mathrm{R}*})$	$\sin\theta_K\sin\theta_l\cos\phi$
16	$\sqrt{\frac{8}{3}}\mathrm{Im}(\mathcal{A}_{\mathrm{S}}^{\mathrm{L}}\mathcal{A}_{\parallel}^{\mathrm{L}*} - \mathcal{A}_{\mathrm{S}}^{\mathrm{R}}\mathcal{A}_{\perp}^{\mathrm{R}*})$	$\sin\theta_K\sin\theta_l\sin\phi$
17	$\sqrt{\frac{2}{3}}\mathrm{Im}(\mathcal{A}_{\mathrm{S}}^{\mathrm{L}}\mathcal{A}_{\perp}^{\mathrm{L}*} + \mathcal{A}_{\mathrm{S}}^{\mathrm{R}}\mathcal{A}_{\perp}^{\mathrm{R}*})$	$\sin\theta_K\sin 2\theta_l\sin\phi$

And what do the amplitudes look like?

[JHEP 0901(2009)019] Altmannshofer et al.

$$\mathcal{A}_0^{\mathrm{L,R}}(q^2) = -8N\frac{m_B m_{K^*}}{\sqrt{q^2}}\left\{\boxed{(C_9 \mp C_{10})}\boxed{A_{12}(q^2)} + \frac{m_b}{m_B + m_{K^*}}\boxed{C_7}\boxed{T_{23}(q^2)} + \boxed{\mathcal{G}_0(q^2)}\right\},$$

$$\mathcal{A}_\parallel^{\mathrm{L,R}}(q^2) = -N\sqrt{2}(m_B^2 - m_{K^*}^2)\left\{\boxed{(C_9 \mp C_{10})}\frac{\boxed{A_1(q^2)}}{m_B - m_{K^*}} + \frac{2m_b}{q^2}\boxed{C_7}\boxed{T_2(q^2)} + \boxed{\mathcal{G}_\parallel(q^2)}\right\},$$

$$\mathcal{A}_\perp^{\mathrm{L,R}}(q^2) = N\sqrt{2\lambda}\left\{\boxed{(C_9 \mp C_{10})}\frac{\boxed{V(q^2)}}{m_B + m_{K^*}} + \frac{2m_b}{q^2}\boxed{C_7}\boxed{T_1(q^2)} + \boxed{\mathcal{G}_\perp(q^2)}\right\},$$

- **$C_{7,9,10}$**: Wilson coefficients
- **A_i**, **T_i**, **V_i**: $B \to K^*$ form factors
- **$G_{\parallel,\perp,0}$**: Charm-loop contribution

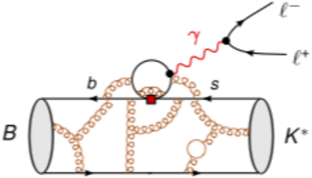

P_5' what?

- Can also reparametrise angular distribution in terms of less form-factor dependent observables (so-called P_i basis) e.g:

$$P_5' \sim \frac{Re(A_0^L A_\perp^{L*} - A_0^R A_\perp^{R*})}{\sqrt{(|A_0^L|^2+|A_0^R|^2)(|A_\perp^L|^2+|A_\perp^R|^2+|A_\parallel^L|^2+|A_\parallel^R|^2)}}$$

- Recent advancements in form-factor calculations coupled with availability of experimental correlations between all observables makes this reparametrisation less important

Acceptance correction

- Trigger, reconstruction and selection efficiency distorts the angular and q^2 distribution of $B^0 \to K^{*0}\mu^+\mu^-$
- Acceptance correction parametrised using 4D Legendre polynomials
- Use moment analysis in $B^0 \to K^{*0}\mu^+\mu^-$ MC to obtain coefficients c_{klmn}
- Measurements in $B^0 \to J/\psi K^{*0}$ control mode in excellent agreemnt with expectation

$$\varepsilon(\cos\theta_\ell, \cos\theta_K, \phi, q^2) = \sum_{klmn} c_{klmn} P_k(\cos\theta_\ell) P_l(\cos\theta_K) P_m(\phi) P_n(q^2)$$

1D projections

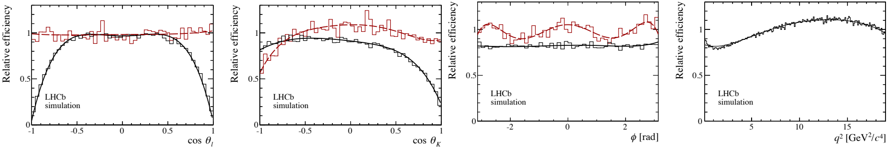

Acceptance correction

- Trigger, reconstruction and selection efficiency distorts the angular and q^2 distribution of $B^0 \to K^{*0}\mu^+\mu^-$
- Acceptance correction parametrised using 4D Legendre polynomials
- Use moment analysis in $B^0 \to K^{*0}\mu^+\mu^-$ MC to obtain coefficients c_{klmn}
- Measurements in $B^0 \to J/\psi K^{*0}$ control mode in excellent agreemnt with expectation

$$\varepsilon(\cos\theta_\ell, \cos\theta_K, \phi, q^2) = \sum_{klmn} c_{klmn} P_k(\cos\theta_\ell) P_l(\cos\theta_K) P_m(\phi) P_n(q^2)$$

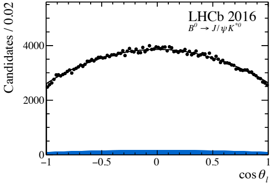

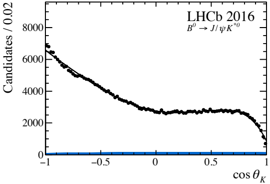

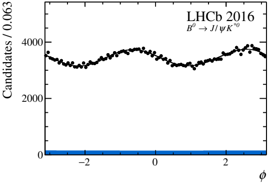

Angular analysis results

Latest update of the 8 CP-averaged observabes using data up to 2016
[Phys. Rev. Lett. 125 (2020) 011802]

Just show a subset here

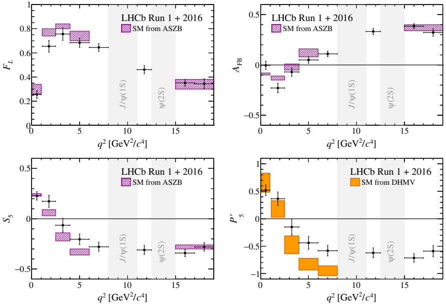

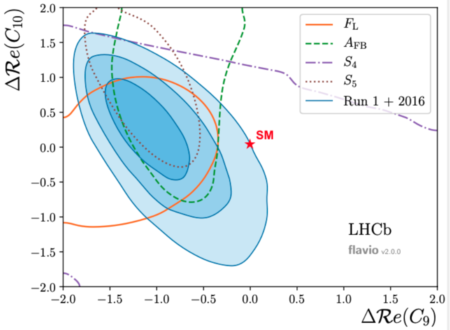

- Suggesting anomalous vector-dilepton coupling (C_9)
- Working on update with twice the data!

Rare decays in Run3 and beyond

- Still have x2 the data to study for most of these analyses just from Run2 alone
  - Much clearer picture in less than 1 year's time
- Angular and LFU measurements statistically limited even after Run3 of the LHC
- Increased dataset → determine theory nuisances directly from the data improving theory accuracy and precision
  - Working with existing data on this

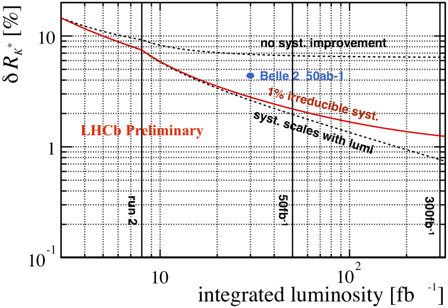

- Larger datasets also bring LHCb's sensitivitiy to τ final states comparable to theory predictions that explain anomalies
  → Smoking gun signatures of anomalies

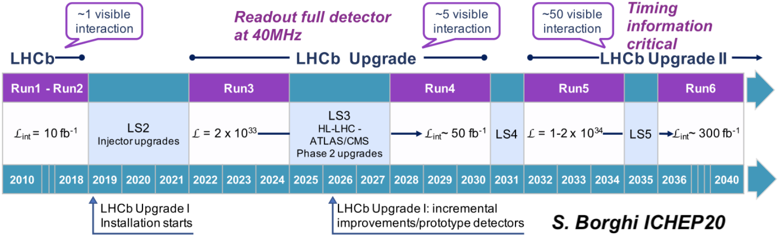

S. Borghi ICHEP20

- Upgrade for Run3 driven by having to read out full detector at 30MHz and higher instantaneous lumi $(4 \times 10^{32} \rightarrow 2 \times 10^{33}\mathrm{cm}^{-2}s^{-1})$
- Fully-software trigger using GPUs for HLT1 and CPUs for HLT2 (RTA before HLT2)
- Upgrade readout electronics of every detector subsystem
- VELO pixels, Sci-Fi tracker, UT silicon strip, new RICH with MaPMT

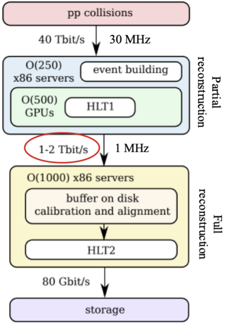

Comput. Softw. Big Sci. (2020) 4, 7
CERN-LHCC-2020-006

Detector performance

[Int.J.Mod.Phys.A30(2015)1530022]

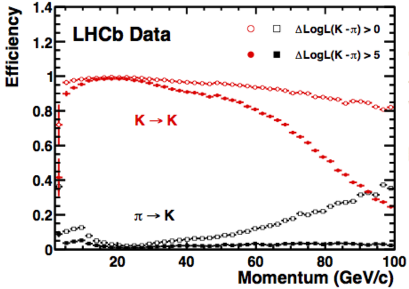

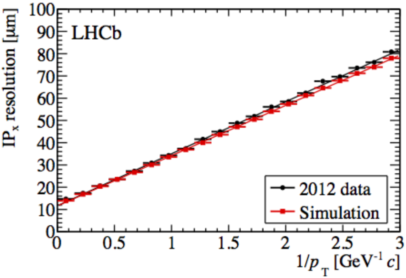

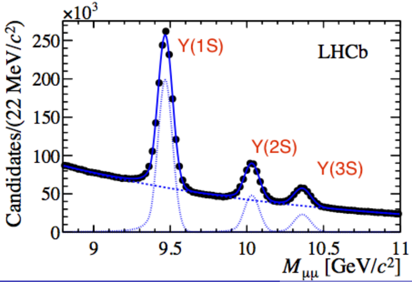

- **Tracking** $\delta p/p = 0.4 - 0.6\%$
- **Muon** $\epsilon_{\mu}^{id} = 98\%$ for 1% mis-id
- Mass resolution $J/\psi \to \mu\mu$
  - LHCb: 13 MeV
  - CMS: 28 MeV [arXiv:1011.4193]
  - ATLAS: 46 MeV [arXiv:1104.3038]